

Effect of Degree of Cross-Linking on Spatial Inhomogeneity in Charged Gels. 3. Ionization Effect

Fumiyoshi Ikkai, Osamu Iritani, and Mitsuhiro Shibayama*

Department of Polymer Science and Engineering, Kyoto Institute of Technology,
Matsugasaki, Sakyo-ku, Kyoto 606-8585, Japan

Charles C. Han

Polymers Division, National Institute of Standards and Technology, Gaithersburg, MD, 20899

Received June 17, 1998; Revised Manuscript Received October 1, 1998

ABSTRACT: The effect of degree of ionization, f , on the spatial inhomogeneities in weakly charged polymer gels has been investigated by light scattering (LS) and small-angle neutron scattering. An anomalous cross-link density (CD) dependence of the scattered intensity, $I(q)$, was observed in a poor solvent (above an inversion temperature, T_{inv}), where q is the scattering vector. That is, a gel became more homogeneous with increasing CD in a poor solvent (above T_{inv}) though it became more heterogeneous with increasing CD in a good solvent (below T_{inv}). LS data indicated the following three features of the gels: (1) an increase of T_{inv} with increasing f , (2) a decrease of the critical degree of polymerization between cross-linking points, N_c , with increasing f , where N_c is the critical value of N at which $I(q)$ diverges with decreasing N ($\sim 1/\text{CD}$), and (3) a decrease of $I(q)$ with f . The influence of f on the anomaly as well as on the microscopic and macroscopic phase separation was discussed in terms of the Rabin-Panyukov (RP) theory proposed for weakly charged gels.

Introduction

The degree of ionization is one of the most important factors to control the microstructure in polymer gels. Many researchers have studied the effect of the degree of ionization on the transparency and swelling properties of polymer gels.^{1–6} These properties are closely connected with many industrial applications, such as contact lenses, solvent absorbents, cosmetics, etc. In general, incorporation of dissociated ionic groups into a neutral polymer gel leads to improvement of transparency and swelling. This phenomenon has been explained as due to the effect of electrostatic repulsion and the Donnan potential.^{2,7–11} The transparency of charged gels has been discussed in relation to their microscopic and macroscopic structural inhomogeneities.^{2,12,13} Since the inhomogeneities are closely connected to spatial concentration fluctuations, scattering methods, such as static light scattering (SLS),^{14–16} dynamic light scattering (DLS),^{3,17,18} small-angle X-ray scattering (SAXS),^{14,19} and small-angle neutron scattering (SANS),^{1,12,20} have been employed to investigate the spatial inhomogeneities in gels.

In our previous papers,^{15,16,20} we discussed an anomalous cross-link density (CD) dependence of the spatial inhomogeneities in an *N*-isopropylacrylamide-*co*-acrylic acid (NIPA/AAc) weakly charged copolymer gel. First,¹⁵ we reported that the ensemble average of scattered intensity, $\langle I(q) \rangle_E$ at a given scattering vector q , increased with CD in a good solvent and decreased with CD in a poor solvent. In the second paper,¹⁶ this inversion phenomenon was reproduced by the Rabin-Panyukov (RP) theory⁵ for weakly charged polymer gels in a poor solvent. According to these findings, we concluded that the inversion, i.e., the anomalous cross-link density dependence, took place as a result of a

competition between two effects of cross-linking: (1) introduction of the static inhomogeneities due to a random distribution of cross-links in the network and (2) suppression of the tendency to a phase-segregated structure due to a pinning effect of cross-links. This conclusion was supported by the SANS result,²⁰ where the inversion of the CD dependence of the scattering intensity, $I(q)$, was reported to take place not only in the LS regime (scattering vector, q , $\approx 0.001 \text{ \AA}^{-1}$) but also in the SANS regime ($0.001 \leq q \leq 0.09 \text{ \AA}^{-1}$).²⁰ To clarify the role of ionized groups on the phase behavior, we study here the effect of degree of ionization, f , on the inversion phenomenon in weakly charged gels.

Experimental Section

Samples. Samples used in this experiment were *N*-isopropylacrylamide/acrylic acid (NIPA/AAc) copolymer gels with different AAc contents. The used ratios of NIPA/AAc molar monomer concentrations were 692/8, 684/16, 668/32, and 636/64. The monomers were dissolved in 40 mL of D₂O including 20 mg of ammonium persulfate (polymerization initiator). The solution was equally divided into eight vessels. Then, the given amounts of *N,N*-methylenebisacrylamide (BIS; cross-linker) were added to each solution. Thus, a series of pregel solutions with BIS concentrations, C_{BIS} , of 0 mM (cross-linking density, CD = 0 mol %), 2 (0.28), 4 (0.57), 6 (0.85), 8 (1.1), 12 (1.7), 16 (2.2), and 24 mM (3.3) were obtained. After adding 24 μL of *N,N,N,N*-tetramethylethylenediamine (TEMED; accelerator), each solution was filtered through a 0.2 μm micropore filter, and gelation was initiated in test tubes at 20 °C. It took about a day for complete gelation. For light scattering (LS) measurements, transparent gels prepared in test tubes were employed without further treatment. For small-angle neutron scattering (SANS) measurements, small gel particles obtained by sifting through a 500 μm sieve were used so as to enhance the rate of thermal equilibration upon a change of temperature. The sifted gels were used for SANS experiments without any further treatment. Each of the gels was placed in a cell with a pair of quartz windows and a rubber O-ring.

* To whom correspondence should be addressed.

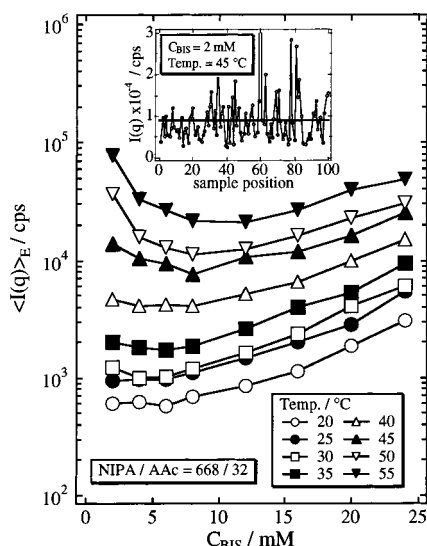


Figure 1. C_{BIS} dependence of $\langle I(q) \rangle_E$ for NIPA/AAc (=668 mM/32 mM) copolymer gels. The inset shows the speckle pattern. The horizontal solid line indicates $\langle I(q) \rangle_E$.

LS. Light scattering (LS) experiments were carried out on a laboratory-made dynamic light scattering instrument with a 10 mW He–Ne laser (wavelength, $\lambda = 6328 \text{ \AA}$) coupled with a photon correlator (DLS-7, Otsuka Electric Co.). The details of the instrument were described elsewhere.²¹ The test tube (the inner diameter, $d = 10 \text{ mm}$) containing a gel was placed in the silicon oil bath whose temperature was controlled within an error of $\pm 0.1 \text{ }^\circ\text{C}$. The light scattering intensity, $I(q)$, was measured at a fixed scattering angle of 60° , where the scattering vector was $q \approx 1.31 \times 10^{-3} \text{ \AA}^{-1}$ ($= (4\pi/\lambda) \sin(\theta/2)$), where n is the refractive index of water. The ensemble average of the scattering intensity, $\langle I(q) \rangle_E$, in the units of count per second (cps) was calculated by measuring $I(q)$'s at 100 different sample positions chosen arbitrarily in the gel. The gel was kept in the bath for more than a day for thermal equilibration before each run. Because $\langle I(q) \rangle_E$'s obtained after 24 and 48 h were found to be roughly identical, we assumed that the gel reached thermal equilibrium within 24 h.

SANS. Small-angle neutron scattering (SANS) experiments were carried out on an 8m-SANS facility (NG1) at the National Institute of Standards and Technology. A neutron beam with a wavelength of 9 \AA irradiated the gel samples in brass cells. The temperature in the cell was changed from 30 to $54 \text{ }^\circ\text{C}$ by a step of $3 \text{ }^\circ\text{C}$. At least 30 min were allowed before each measurement in order to ensure thermal equilibrium. The absolute scattering intensity functions, $I(q)$, at $0.01 \leq q \leq 0.09 \text{ \AA}^{-1}$ were obtained by the following procedure. The scattered neutrons were counted with a two-dimensional detector and were circularly averaged by taking account of the detector inhomogeneities, followed by correction for cell scattering, fast neutrons, and transmission. Then, $I(q)$ in the absolute intensity scale was obtained by multiplying the scaling factor determined with a Lupolen standard. No noticeable difference was observed in $I(q)$'s between the sifted gels and the corresponding one-piece gels.

Results and Discussion

1. Anomalous Cross-Link Density Dependence.

Figure 1 shows the C_{BIS} dependence of $\langle I(q) \rangle_E$ for (N-isopropylacrylamide/acrylic acid) (NIPA/AAc) copolymer gels with NIPA/AAc = 668 mM/32 mM. Here, $\langle I(q) \rangle_E$ was obtained by averaging light scattered intensities at 100 different sample positions arbitrarily chosen in the gel. The inset shows the scattered intensity variation with sample positions, i.e., so-called a speckle pattern, and the horizontal solid line indicates $\langle I(q) \rangle_E$. Ideally, the degree of heterogeneity should be defined

by the ratio $\langle I \rangle_E / \langle I \rangle_F$, where $\langle I \rangle_F$ is the scattering intensity originated from the thermal fluctuations. This ratio normalizes the intensity of the incident beam. However, we employed the value of $\langle I \rangle_E$ in this study since the incident beam intensity was confirmed to be roughly constant during the experiment. $\langle I(q) \rangle_E$ increases with C_{BIS} at low temperatures up to $40 \text{ }^\circ\text{C}$. However, $\langle I(q) \rangle_E$ becomes a concave function of C_{BIS} for $T \geq 45 \text{ }^\circ\text{C}$, having a minimum around $C_{\text{BIS}} \approx 8 \text{ mM}$. In the previous papers, we called this kind of opposite C_{BIS} dependence in $\langle I(q) \rangle_E$ the *inversion* (or *anomaly*), and concluded that this inversion occurs due to the competition between two effects of cross-linking.^{15,16} The physical meaning of the inversion was already given in the Introduction.

Figure 2 shows the N dependence of $\langle I(q) \rangle_E$'s at different degrees of ionization, f , i.e., $f = 0.011$ (NIPA/AAc = 692/8), 0.023 (=684/16), 0.046 (=668/32), and 0.091 (=636/64), where N is the nominal degree of polymerization between cross-linking points. The value of N was estimated by assuming complete reaction of monomers and cross-linkers, i.e., $N = (C_{\text{NIPA}} + C_{\text{BIS}}) / C_{\text{BIS}}$. Roughly speaking, N is inversely proportional to CD when $C_{\text{BIS}} \ll C_{\text{NIPA}}$. Figure 2 indicates three important features: (1) The inversion temperature, T_{inv} , i.e., the lowest temperature where an inversion in $\langle I(q) \rangle_E$ with respect to N takes place, increases with increasing f , i.e., $T_{\text{inv}} = 37$ (for $f = 0.011$), 40 ($f = 0.023$), 45 ($f = 0.046$), and $45 \text{ }^\circ\text{C}$ ($f = 0.091$). (2) The $\langle I(q) \rangle_E$ curves shift downward with increasing f . (3) A divergence of $\langle I(q) \rangle_E$ takes place with decreasing N . This divergence is known as the cross-link saturation threshold, where the length scale associated with static inhomogeneities diverges.²²

We now compare the behavior of $\langle I(q) \rangle_E$ shown in Figure 2 with a theory for weakly charged polymer gels, i.e., the Rabin–Panyukov (RP) theory.⁵ The RP theory takes account of the two opposite interactions, i.e., the electrostatic (repulsive) interaction and the hydrophobic (attractive) interaction. The structure factor, $S(q)$, for instantaneously cross-linked networks of Gaussian phantom chains with excluded volume is given by

$$S(q) = G(q) + C(q) \quad (1)$$

where $G(q)$ and $C(q)$ are correlators of the thermal fluctuations and of the static density inhomogeneities, respectively. These are given by

$$G(q) = \frac{\phi N g(q)}{1 + w(q)g(q)} \quad (2)$$

$$C(q) = \frac{\phi N}{[1 + w(q)g(q)]^2 (1 + Q^2)^2} \times \left[6 + \frac{9}{w_0(q) - 1 + (1/2)Q^2(\phi_0/\phi)^{2/3}\phi_0^{-1/4}} \right] \quad (3)$$

where a , N , ϕ , f , and $w(q)$ indicate the segment length (8.12 \AA for NIPA polymer chains^{12,23}), the average degree of polymerization between cross-links, the network volume fraction, the degree of ionization, and the effective second virial coefficient, respectively. The parameters with and without the subscript 0 denote those of the initial state and the final state, respectively. Q ($= aN^{1/2}q$) is the dimensionless wave vector. The function $g(q)$ is given by

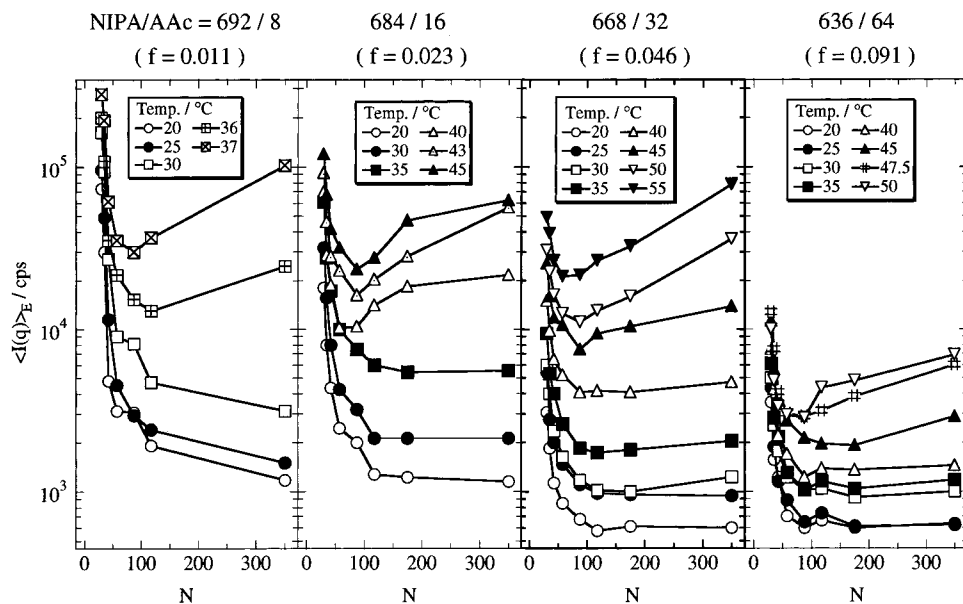


Figure 2. N dependence of $\langle I(q) \rangle_E$'s at different f s, i.e., $f = 0.011$ (NIPA/AAc = 692/8), 0.023 (=684/16), 0.046 (=668/32), and 0.091 (=636/64) and at different temperatures.

$$g(q) = \frac{1}{Q^2/2 + (4Q^2)^{-1} + 1} + \frac{2(\phi/\phi_0)^{2/3}\phi_0^{1/4}}{(1 + Q^2)^2} \quad (4)$$

The functions, $w(q)$ and $w_0(q)$, are expressed by

$$w(q) = (1 - 2\chi + \phi)\phi N + \frac{I_B f^2 \phi N^2}{Q^2 + I_B f \phi N} \quad (\text{poor solvent}) \quad (5)$$

$$w_0(q) = \phi_0^{5/4} N + \frac{I_B f_0^2 \phi_0^{5/4} N^2}{Q^2 (\phi_0/\phi)^{2/3} + I_B f_0 \phi_0^{5/4} N} \quad (\text{good solvent}) \quad (6)$$

where χ is the Flory interaction parameter and the initial state is assumed to be in a good solvent (the scaling) regime (eq 6). On the other hand, the final state is taken as a poor solvent regime (eq 5).⁵ I_B is the dimensionless Bjerrum length given by $I_B = 4\pi L_B/a$, where L_B is the Bjerrum length. In this paper, L_B is fixed to 7 Å, i.e., the value for aqueous solutions at 25 °C.¹²

Figure 3 shows theoretical predictions for $S(q)$ obtained with the same parameters for the gels discussed in Figure 2. Only the χ parameter was chosen arbitrarily in order to reproduce the N dependence. Here, $S(q)$ is calculated from eq 1 at $q = 0.001 \text{ Å}^{-1}$ corresponding to the scattering angle of LS at 60°. As shown in this figure, $\langle I(q) \rangle_E$'s in Figure 2 are satisfactorily reproduced by the theoretical lines of $S(q)$. The figures indicate that χ_{inv} , i.e., the χ value where an inversion of $S(q)$ takes place with respect to N , increases from about 0.58 to 1.10 with increasing f from 0.011 to 0.091. Also, the higher the value of f , the lower is the $S(q)$.

2. Inversion vs Phase Separation. Figure 4 shows a series of phase diagrams for the inversion calculated from RP theory at (a) $q = 0.001 \text{ Å}^{-1}$ (LS region) and (b) $q = 0.02 \text{ Å}^{-1}$ (SANS region). The solid lines in the figure indicate the ϕ dependence of χ_{inv} for various f s. These lines were obtained numerically as the point where $[\partial S(q)/\partial N]_{q^*, N=100}$ changes sign, at $q^* = 0.001 \text{ Å}^{-1}$ (for LS) and 0.02 Å^{-1} (for SANS), respectively.

On the other hand, the dotted lines indicate the critical values of χ and χ_c , i.e., the coexistence curve at which phase separation takes place. This curve was obtained by imposing the condition, $S(q) \rightarrow \infty$ and $N \gg 1$, which is given by¹⁶

$$\chi_c = \frac{1}{2} \left(1 + \phi + \frac{f}{\phi} \right) \quad (7)$$

From the figures, it is found that the ϕ dependence of χ_{inv} is similar to that of χ_c . Note that the curves for χ_c 's are the same in both (a) and (b) irrespective of the q range. However, a more careful observation reveals a q dependence of χ_{inv} . In particular, for $f < 0.023$, the deviation of the inversion lines for $q = 0.001 \text{ Å}^{-1}$ (LS regime) from those for $q = 0.02 \text{ Å}^{-1}$ (SANS regime) becomes significant. As shown in Figure 4b, the inversion line (solid line) is above the coexistence curve (dotted line) only in the case of $f = 0$. For $f \neq 0$, on the other hand, the inversion line is always below the coexistence curve. This means that, for weakly charged gels (i.e., $f \neq 0$), the system first encounters an inversion border and then enters a phase-separated region with increasing χ .

On the other hand, as shown in Figure 4a, an inversion in the N dependence of $S(q)$ is always expected for $f = 0$ in the LS regime irrespective of the value of ϕ . This fact, i.e., the presence of a q dependence for the inversion phenomenon, suggests that the relative contribution of the spatial frozen inhomogeneities in the gel to the net scattering varies as a function of q . This can be better understood by plotting the f dependence of χ_c (phase separation) or χ_{inv} .

Figure 5a shows the f dependence of χ_c (phase separation). Here, N and ϕ were fixed to 100 and 0.07, respectively. In the figure are also shown the lines for the inversion, χ_{inv} , at $q = 0.001$ and 0.02 Å^{-1} . By comparison of χ_c with χ_{inv} ($q = 0.02 \text{ Å}^{-1}$), it can be deduced that an inversion phenomenon is expected for $f \geq 0.01$, as indicated with an arrow. On the other hand, such an inversion is always expected in the LS regime since the curves of χ_c and χ_{inv} ($q = 0.001 \text{ Å}^{-1}$) do not cross each other and the χ_{inv} curve is always below that

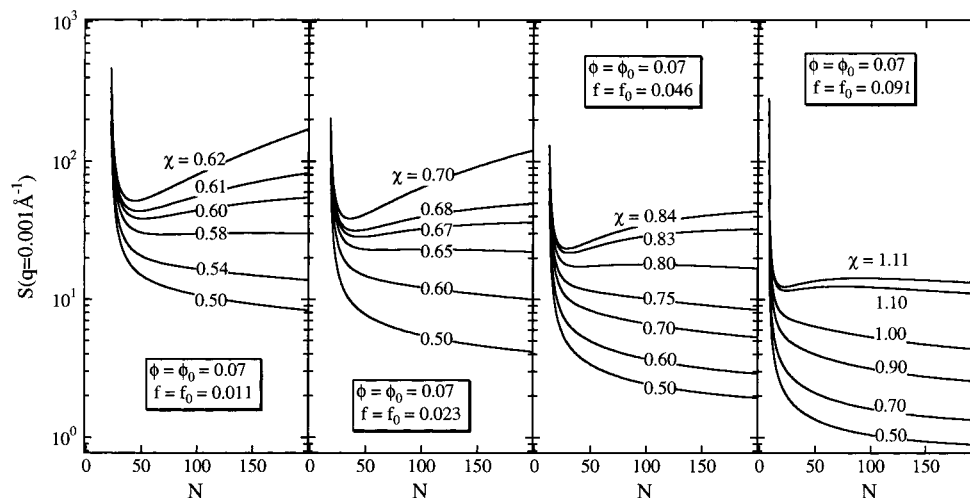


Figure 3. Theoretical predictions obtained with the same parameters for the gels discussed in Figure 2, where only the value of the χ parameter was chosen in order to reproduce Figure 2.

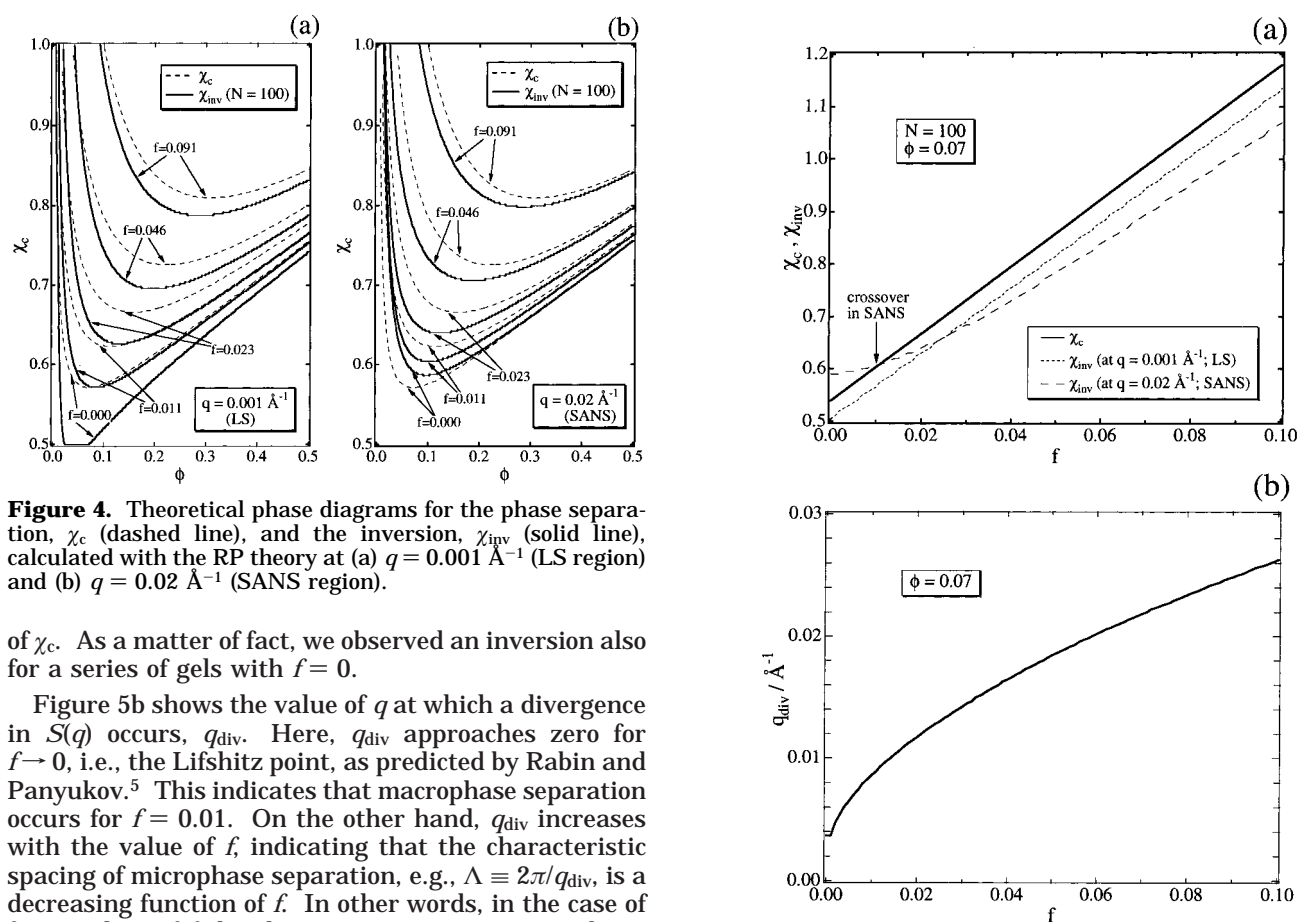


Figure 4. Theoretical phase diagrams for the phase separation, χ_c (dashed line), and the inversion, χ_{inv} (solid line), calculated with the RP theory at (a) $q = 0.001 \text{ \AA}^{-1}$ (LS region) and (b) $q = 0.02 \text{ \AA}^{-1}$ (SANS region).

of χ_c . As a matter of fact, we observed an inversion also for a series of gels with $f = 0$.

Figure 5b shows the value of q at which a divergence in $S(q)$ occurs, q_{div} . Here, q_{div} approaches zero for $f \rightarrow 0$, i.e., the Lifshitz point, as predicted by Rabin and Panyukov.⁵ This indicates that macrophase separation occurs for $f = 0.01$. On the other hand, q_{div} increases with the value of f , indicating that the characteristic spacing of microphase separation, e.g., $\Lambda \equiv 2\pi/q_{div}$, is a decreasing function of f . In other words, in the case of finite values of f , the phase separation is restricted in a microscopic scale because ionic groups present in the gel depress concentration fluctuations with long wavelengths. Hence, a microphase separation, i.e., a phase separation with a finite Λ , takes place instead of a macrophase separation ($\Lambda \rightarrow 0$).

Figure 6 shows the q dependence of $S(q)$. All parameters except the value of f and χ were chosen the same as in the experiment. The inversion is demonstrated here as a crossover of $S(q)$'s for $N = 80$ and 200 . For $f = 0$ (Figure 6a,b), $S(q)$ indicates that an inversion occurs at small q regions ($q < 0.01 \text{ \AA}^{-1}$, in this particular case). For $f = 0.0457$ (Figure 6c,d), on the other hand, $S(q)$ shows an inversion by increasing χ around $q = 0.02 \text{ \AA}^{-1}$.

Figure 5. (a) f dependence of χ_c (phase separation) and χ_{inv} (inversion). (b) f dependence of the q value at which divergence in $S(q)$ occurs, q_{div} .

The predicted structure factors in Figure 6 can be compared with experimental results. Figure 7 shows the N dependence of the scattering intensity $I(q)$ for NIPA/AAc (668/32; $f = 0.0457$) gels obtained by SANS. As discussed in Figure 6b and in the previous paper,²⁰ $I(q)$ decreases with decreasing N at $q \approx 0.02 \text{ \AA}^{-1}$. Therefore, the presence of a q dependence predicted by the theory is now confirmed. Another interesting feature in Figure 7 is the crossover of $I(q)$'s at $q \approx 0.03 \text{ \AA}^{-1}$. As a matter of fact, all of the $I(q)$'s in Figure 7

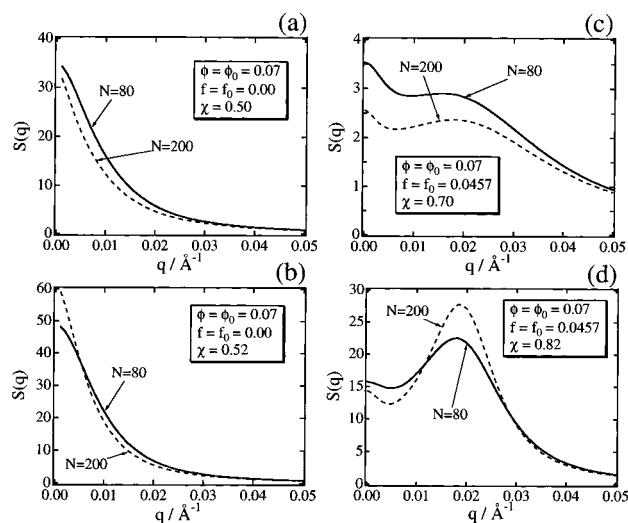


Figure 6. $S(q)$'s calculated for the cases of $N = 80$ and 200 .

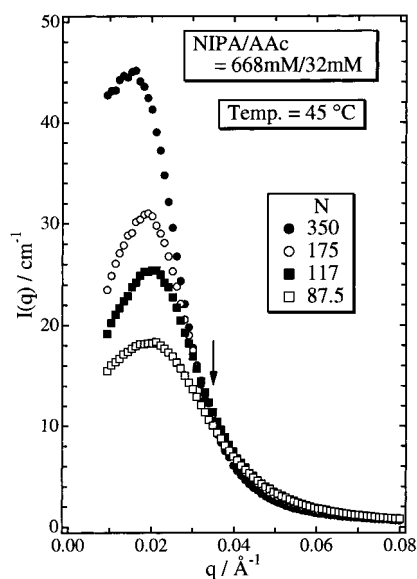


Figure 7. N dependence of SANS intensity curves, $I(q)$, for NIPA/AAC (668/32). The arrow indicates the q value where a crossover of $I(q)$ occurs.

merge at $q \approx 0.03 \text{ \AA}^{-1}$ (indicated with an arrow), above which no anomaly occurs. The RP theory also indicates that inversion never takes place for $q \geq 0.03 \text{ \AA}^{-1}$. This suggests that the lower bound for the characteristic spacing required for microphase separation lies around the spatial order of $1/0.03 \text{ \AA}^{-1}$ (ca. 200 \AA). However, the physical meaning of this criterion is still an open question.

Conclusions

The effect of degree of ionization, f , in a weakly charged copolymer gel on the inversion of N dependence

in $S(q)$ was investigated by light scattering (LS) and small-angle neutron scattering (SANS). It was shown that the ionic groups present in polymer gels play a decisive role to determine the state of the spatial inhomogeneities. The effect of f on gel inhomogeneities was discussed in details in terms of three types of phenomena, i.e., inversion, and micro- and macrophase separations. It was concluded that an inversion phenomenon is expected for $f \geq 0.01$ in the SANS regime. On the other hand, such an inversion is expected in the LS regime even for neutral gels ($f = 0$).

Acknowledgment. F.I. acknowledges the Research Fellowship of the Japan Society for the Promotion of Science for Young Scientists. This work is partially supported by the Ministry of Education, Science, Sports, and Culture, Japan (Grants-in-Aid, Nos. 09450362 and 10875199 to M.S.).

References and Notes

- (1) Schosseler, F.; Skouri, R.; Munch, J. P.; Candau, S. J. *J. Phys. II* **1994**, *4*, 1221.
- (2) Shibayama, M.; Ikkai, F.; Inamoto, S.; Nomura, S.; Han, C. C. *J. Chem. Phys.* **1996**, *105*, 4358.
- (3) Shibayama, M.; Fujikawa, Y.; Nomura, S. *Macromolecules* **1996**, *29*, 6535.
- (4) Borue, V.; Erukhimovich, I. *Macromolecules* **1988**, *21*, 3240.
- (5) Rabin, Y.; Panyukov, S. *Macromolecules* **1997**, *30*, 301.
- (6) Sasaki, S.; Maeda, H. *J. Chem. Phys.* **1997**, *107*, 1028.
- (7) Flory, P. J. *Principles in Polymer Chemistry*; Cornell University: Ithaca, NY, 1953.
- (8) Lifshitz, I. M.; Grosberg, A. Y.; Khokhlov, A. R. *Rev. Modern Phys.* **1978**, *50*, 683.
- (9) Shibayama, M.; Uesaka, M.; Shiwa, Y. *J. Chem. Phys.* **1996**, *105*, 4350.
- (10) Hooper, H. H.; Baker, H. P.; Blanch, H. W.; Prausnitz, J. M. *Macromolecules* **1990**, *23*, 1096.
- (11) Richa, J.; Tanaka, T. *Macromolecules* **1984**, *17*, 2916.
- (12) Shibayama, M.; Tanaka, T.; Han, C. C. *J. Chem. Phys.* **1992**, *97*, 6842.
- (13) Shibayama, M. *Macromol. Chem. Phys.* **1998**, *199*, 1.
- (14) Mallam, S.; Horkay, F.; Hecht, A. M.; Geissler, E. *Macromolecules* **1989**, *22*, 3356.
- (15) Ikkai, F.; Shibayama, M. *Phys. Rev. E* **1997**, *56*, R51.
- (16) Shibayama, M.; Ikkai, F.; Shiwa, Y.; Rabin, Y. *J. Chem. Phys.* **1997**, *107*, 5227.
- (17) Shibayama, M.; Takata, T.; Norisuye, T. *Physica A* **1998**, *249*, 245.
- (18) Shibayama, M.; Norisuye, T.; Nomura, S. *Macromolecules* **1996**, *29*, 8746.
- (19) Cohen, Y.; Ramon, O.; Kopelman, I. J.; Mizrahi, S. *J. Polym. Sci., Polym. Phys. Ed.* **1992**, *30*, 1055.
- (20) Ikkai, F.; Shibayama, M.; Han, C. C. *Macromolecules* **1998**, *31*, 3275.
- (21) Shibayama, M.; Takeuchi, T.; Nomura, S. *Macromolecules* **1994**, *27*, 5350.
- (22) Panyukov, S.; Rabin, Y. *Phys. Rep.* **1996**, *269*, 1.
- (23) Kubota, K.; Fujishige, S.; Ando, I. *Polym. J.* **1990**, *22*, 15.

MA980962E